Shell model study of the high spin states in the $N=50$ isotones ^{92}Mo, ^{93}Tc, ^{94}Ru, and ^{95}Rh

S. S. Ghugre
Department of Physics, University of Notre Dame, Notre Dame, Indiana 46556

S. K. Datta
Nuclear Science Center, Aruna Asaf Ali Marg, P.O. Box 10502, New Delhi 110 067, India
(Received 3 April 1995)

The low lying levels in $N=50$ isotones have been well described within the shell model framework. These calculations were performed assuming an inert neutron core and the valence protons occupying either the $(p_{1/2},g_{9/2})$ or $(f_{5/2},p_{3/2},p_{1/2},g_{9/2})$ orbits. With the advent of multidetector arrays the level schemes of these nuclei have been extended to high spin regimes $(J=20-25\hbar)$. The inclusion of neutron core excitation (neutron particle-hole excitation across the $N=50$ shell gap) was essential to adequately describe these observed higher angular momentum states. Calculations involving neutron particle-hole excitation across the $N=50$ shell gap, coupled to the lower valence proton configurations, were not feasible due to computational limitations. This paper describes a truncation scheme devised to perform large basis shell model calculations. The level sequences observed in the $N=50$ isotones ^{92}Mo, ^{93}Tc, ^{94}Ru, and ^{95}Rh are interpreted on the basis of the shell model calculations in the configuration space $f_{5/2}$, $p_{3/2}$, $p_{1/2}$, $g_{9/2}$ for the protons and $p_{1/2}$, $g_{9/2}$, $g_{7/2}$, $d_{5/2}$, $d_{3/2}$, $s_{1/2}$ for the neutrons. The excitation of a $g_{9/2}$ neutron across the $N=50$ shell, into the next major oscillator shell describes the observed higher angular momentum states in these nuclei.

PACS number(s): 21.60.Cs, 27.60.+j

I. INTRODUCTION

The $N=50$ nuclei (^{92}Mo, ^{93}Tc, ^{94}Ru, ^{95}Rh) have attracted physicists since the first developments of the nuclear shell model. The low-lying levels in these nuclei ($N=50$, $Z=40-50$) have been well described within the shell model framework using ^{88}Sr as the inert core and the $p_{1/2},g_{9/2}$ model space [1–3]. Ji and Wildenthal [4] used ^{78}Ni as the closed core and the valence $f_{5/2},p_{3/2},p_{1/2},g_{9/2}$ proton orbitals to study the $N=50$ isotones from ^{78}Ni to ^{100}Sn. Recent calculations by Sinatkas *et al.* [5] used ^{100}Sn as the core and the valence proton holes in the $f_{5/2},p_{3/2},p_{1/2},g_{9/2}$ orbits to study the level structures in these nuclei. However, all these calculations had assumed an inert neutron core.

All the above mentioned calculations were restricted to the low-lying levels, due to the absence of experimental data on the higher angular momentum states. With the advent of modern Compton-suppressed HPGe detector arrays, it is now possible to extend the yrast level schemes of these nuclei to higher spin regimes ($J=22\hbar$) [6–8]. There exist two mechanisms for the generation of the observed higher angular momentum states: (i) promoting the protons from the $(f_{5/2},p_{3/2})$ orbits into the $g_{9/2}$ orbit and (ii) the excitation of a neutron across the $N=50$ shell closure. Hence to adequately describe the observed higher angular momentum states in these nuclei the shell model calculations have to be performed within a model space that encompasses both these mechanisms. The shell model calculations have to be performed in a configuration space consisting of the $(f_{5/2},p_{3/2},p_{1/2},g_{9/2})$ proton orbits and the $(p_{1/2},g_{9/2},d_{5/2})$ neutron orbits to interpret the level sequences in these nuclei up to a spin of about $J=(20-25)\hbar$. However, such large basis unrestricted calculations are not feasible due to computational limitations. For example the coupling of one $\nu(g_{9/2})$ hole to the protons in the fpg subspace would result in dimensions of the Hamiltonian matrices of about 10 000. Thus a truncation scheme would have to be developed to perform such large basis calculations.

II. TRUNCATION SCHEME

Because of computational difficulties, large basis shell model calculations have to be performed within a space truncated from the desired model space. Truncation of model space is not a trivial task. The single-particle energies and the effective interactions are model space dependent. Hence these would have to be renormalized to include the effect of the truncated orbits. This renormalization process is a hugely difficult task. It is desirable to devise a truncation scheme wherein this complicated renormalization process did not play a significant part, and the original effective interactions could be used.

Other workers reported various truncation schemes employed in the $A=90$ mass region. Ji and Wildenthal [4] devised a truncation scheme to describe the low-lying levels of $N=50$ isotones from ^{78}Ni to ^{100}Sn. They internally truncated the $f_{5/2},p_{3/2},p_{1/2},g_{9/2}$ model space by restricting only a maximum of four particles to be excited across the ^{90}Zr Fermi surface (into the $g_{9/2}$ orbit). The major disadvantage of this scheme is that it is not applicable to any other model space. Kabadiyski *et al.* [9] reported the study of the high spin states in ^{90}Mo using a model space consisting of the proton $(f_{5/2},p_{3/2},p_{1/2},g_{9/2})$ orbits and the neutron $(p_{1/2},g_{9/2},g_{7/2},d_{5/2},d_{3/2},s_{1/2})$ orbits outside ^{66}Ni as the core. Truncation was made using the method designated by Brussard and Glaudemans [10]. In this method all possible configurations and the resultant excitation energies within the given model space were computed. All those configurations which result in an excitation energy above a certain cutoff value were not included in the calculations. The advantage of

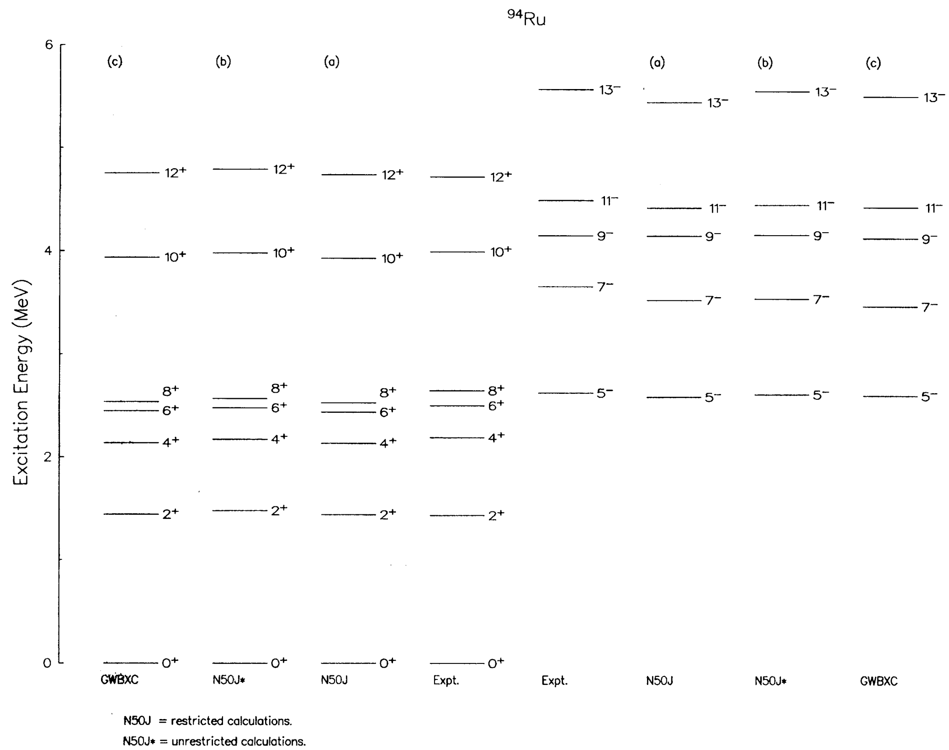

FIG. 1. Comparison of the observed states up to $J=12\hbar$ in ^{94}Ru with the spherical shell model calculations, using different model spaces.

this scheme was its simplicity. However, this scheme has the disadvantage that all possible configurations had to be worked out *a priori*, which is not an easy task within a large model space.

It is desirable that the truncation scheme should be applicable to any model space under consideration, and preferably should not involve complicated calculations. Before we set up our truncation scheme we define a term "partition," such that a partition P is a set of occupancies for the orbits under consideration. When the calculations are carried out within a large model space, the wave function for any state consists of a large number of partitions (configurations) arising from the distribution of the valence particles within the available orbits. However, of these several configurations, only a few would contribute significantly to the wave function of a state under consideration; i.e., a given angular momentum state would have only a few dominant configurations. The model space could then be internally truncated by considering only these dominant configurations in the calculations. It is expected that the calculations performed in a truncated model space would differ slightly from the results obtained from the full (unrestricted) model space, if we have made the correct guess as regards the choice of the dominant configurations. Initially one would have to guess these dominant configurations to begin with. Several iterations would be required to obtain the final dominant configurations. However, if the starting guess configurations were as good a guess to the final solutions, several intermediate steps could be done away with. This is possible if one were to use the results from model spaces, which are small enough to perform unrestricted calculations.

The main advantage of this scheme is that since we have considered only the dominant configurations for a particular state, we need not renormalize the effective interaction to include the effect of the neglected configurations. This is due to the fact that the contributions from these neglected configurations would be extremely negligible. A point worth mentioning is that, since we perform the calculations for the most dominant configurations, these configurations essentially correspond to energetically favorable states. Hence our truncation scheme is very similar to the one devised by Kabadiyski *et al.* [9], except the fact that the number of parti-

TABLE I. $B(E2)$ values for the low-lying levels (up to $J=12^+\hbar$) in ^{94}Ru. The $B(E2)$ values are given in units of e^2 fm^4. In the calculations effective charges of 1.98 and 1.78 have been used for the protons and neutrons, respectively.

$J_i \rightarrow J_f$	$B(E2)$ [a]	$B(E2)$ [b]	$B(E2)$ [c]	$B(E2)$ [d]
$2^+ \rightarrow 0^+$	241.2	233.8	246.0	282
$4^+ \rightarrow 2^+$	2.7	2.9	2.0	2.0
$6^+ \rightarrow 4^+$	5.5	5.9	5.6	6.0
$8^+ \rightarrow 6^+$	0.9	1.0	0.9	0.9
$10^+ \rightarrow 8^+$	179.4	179.9	183.0	209
$12^+ \rightarrow 10^+$	95.3	95.6	91.1	104

[a]Wave functions from the unrestricted calculations using N50J model space. Refer to the text for details on the N50J model space.
[b]Wave functions obtained from the calculations performed within the truncated N50J model space.
[c]Wave functions from the calculations performed within the truncated GWB model space. Refer to the text for details on this model space.
[d]Values obtained from the work of Ji and Wildenthal.

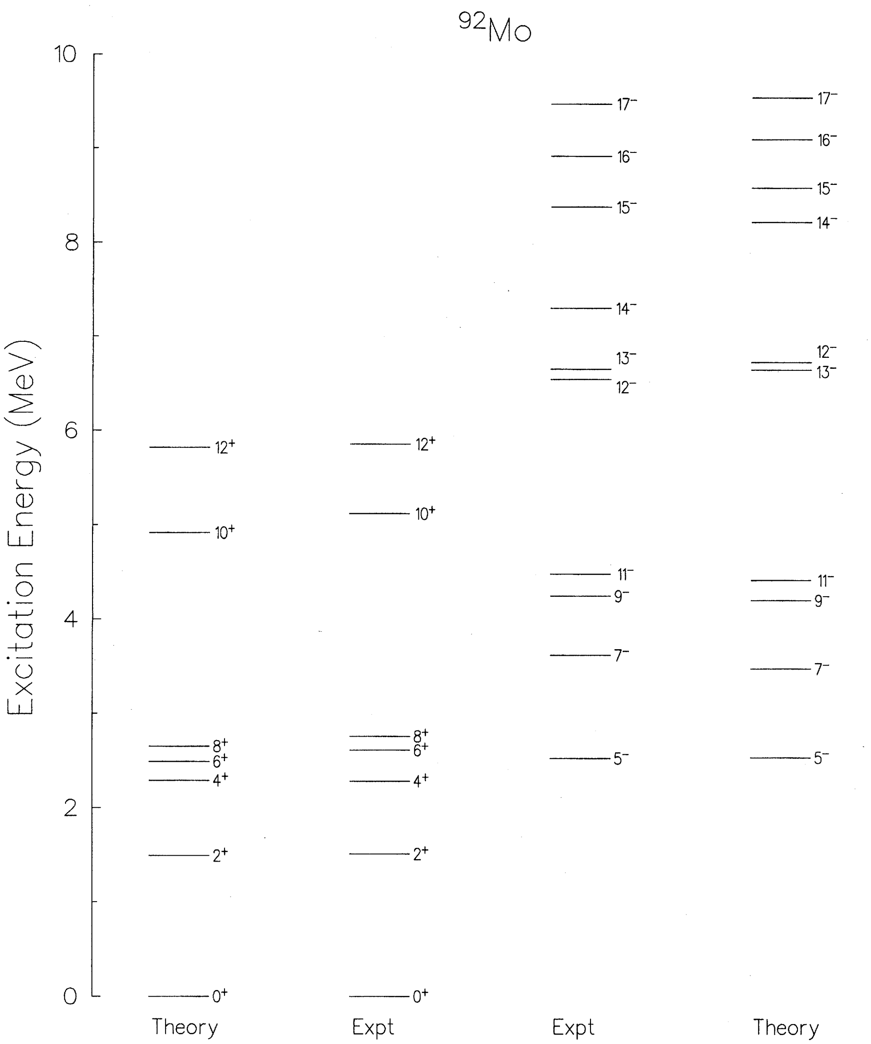

FIG. 2. Comparison of the experimental and calculated excitation energies in ^{92}Mo with the shell model predictions.

tions considered is essentially governed by our existing computational limitations. The only disadvantage of our scheme could be that one will have to initially guess the dominant configurations.

The shell model calculations have been performed using the code OXBASH [11]. In this code, truncation can be made by selecting out the partitions (configurations) to be included in the calculations. We decided to test the truncation scheme for a case where we would be in a position to compare the results obtained from our truncated calculations with the results from unrestricted calculations. For this reason we choose the model space used by Ji and Wildenthal [4], with active $(f_{5/2},p_{3/2},p_{1/2},g_{9/2})$ proton orbits outside the ^{78}Ni as the core. The effective interaction and the single-particle energies are similar to the ones used by Ji and Wildenthal [4]. This model space and the corresponding interaction were code named N50J in the code OXBASH [11].

We performed the test calculations for ^{94}Ru. ^{94}Ru has 16 valence protons outside the ^{78}Ni core. The levels up to a spin of $I=12^+$ and 13^- would be dominated by the valence protons in the fpg subspace. These states would not have any contribution from the excitation of the neutron core. A particular wave function would be composed in general of many partitions, where each partition is of the form $P=[\pi(p(1),p(2),p(3),p(4))]$ where $p(i)$ represents the number of protons in the $f_{5/2},p_{3/2},p_{1/2},g_{9/2}$ orbits, respectively. This enabled us to choose the partitions $P(1)$ and $P(2)$ for the positive and negative parity bands for levels up to $I=12^+$ and 13^-. The list of partitions is given below: $P(1) = \pi(6,4,2,4) = \pi(6,4,0,6) = \pi(6,3,1,6) = \pi(6,2,2,6) = \pi(5,4,1,6) = \pi(5,3,2,6) = \pi(4,4,2,6)$ and $P(2) = \pi(6,4,1,5) = \pi(6,3,2,5) = \pi(6,3,0,7) = \pi(6,2,1,7) = \pi(5,4,2,5) = \pi(5,2,2,7) = \pi(4,4,1,7)$.

It is expected that configurations arising from the excitation of more than two particles from the $p_{3/2}$ orbit and more than four particles from the $f_{5/2}$ orbit would result in a higher excitation energy for a given state and hence were not considered in our calculations. The comparison of the experimental [8] and calculated level energies for ^{94}Ru up to a spin of $I=12^+$ and 13^- is shown in Fig. 1(a). The excitation energies of all experimentally known yrast states up to $I=12^+$ and 13^- are well reproduced in the calculations. Unrestricted calculations for the above mentioned states (all

TABLE II. Main partitions of wave functions for ^{92}Mo. The wave function for a particular angular momentum state would be composed of several partitions, where each partition is of the form $P=[\pi(p(1),p(2),p(3),p(4))\otimes\nu(n(1),n(2),n(3))]$, where $p(i)$ represents the number of protons occupying the $f_{5/2}$, $p_{3/2}$, $p_{1/2}$, and $g_{9/2}$ orbits, and $n(j)$ represents the number of neutrons in the $p_{1/2}$, $g_{9/2}$, and $d_{5/2}$ orbits, respectively. In these calculations no neutrons were allowed to be excited to the $g_{7/2}$, $d_{3/2}$, and $s_{1/2}$ orbits.

J ($\hbar$)	Energy (keV)	Wave function π	Seniority ν	Partitions (%)
2^+	1510	$\pi(6,4,2,2)\otimes\nu(2,10,0)$	0	65.37%
		$\pi(6,4,0,4)\otimes\nu(2,10,0)$	0	15.41%
		$\pi(6,2,2,4)\otimes\nu(2,10,0)$	0	10.53%
4^+	2282	$\pi(6,4,2,2)\otimes\nu(2,10,0)$	0	69.31%
		$\pi(6,4,0,4)\otimes\nu(2,10,0)$	0	14.50%
		$\pi(6,2,2,4)\otimes\nu(2,10,0)$	0	10.02%
6^+	2611	$\pi(6,4,2,2)\otimes\nu(2,10,0)$	0	69.14%
		$\pi(6,4,0,4)\otimes\nu(2,10,0)$	0	14.34%
		$\pi(6,2,2,4)\otimes\nu(2,10,0)$	0	9.67%
8^+	2759	$\pi(6,4,2,2)\otimes\nu(2,10,0)$	0	70.44%
		$\pi(6,4,0,4)\otimes\nu(2,10,0)$	0	14.63%
		$\pi(6,2,2,4)\otimes\nu(2,10,0)$	0	9.56%
10^+	5120	$\pi(6,4,0,4)\otimes\nu(2,10,0)$	0	50.30%
		$\pi(5,4,1,4)\otimes\nu(2,10,0)$	2	19.84%
		$\pi(4,4,2,4)\otimes\nu(2,10,0)$	0	14.32%
12^+	5859	$\pi(6,4,0,4)\otimes\nu(2,10,0)$	0	63.14%
		$\pi(6,3,1,4)\otimes\nu(2,10,0)$	2	10.15%
		$\pi(5,4,1,4)\otimes\nu(2,10,0)$	2	10.19%
5^-	2526	$\pi(6,4,1,3)\otimes\nu(2,10,0)$	2	84.51%
7^-	3623	$\pi(6,4,1,3)\otimes\nu(2,10,0)$	2	65.37%
		$\pi(5,4,2,3)\otimes\nu(2,10,0)$	2	13.42%
		$\pi(6,3,2,3)\otimes\nu(2,10,0)$	2	10.31%
9^-	4249	$\pi(6,4,1,3)\otimes\nu(2,10,0)$	2	78.77%
		$\pi(6,3,2,3)\otimes\nu(2,10,0)$	2	11.68%
11^-	4483	$\pi(6,4,1,3)\otimes\nu(2,10,0)$	2	85.40%
12^-	6547	$\pi(5,4,2,3)\otimes\nu(2,10,0)$	2	85.22%
13^-	6657	$\pi(5,4,2,3)\otimes\nu(2,10,0)$	2	
		$\pi(5,4,0,5)\otimes\nu(2,10,0)$	2	23.02%
14^-	7306	$\pi(6,4,1,3)\otimes\nu(2,9,1)$	4	63.90%
		$\pi(6,3,2,3)\otimes\nu(2,9,1)$	4	21.22%
		$\pi(5,4,2,3)\otimes\nu(2,9,1)$	4	12.84%
15^-	8381	$\pi(6,4,1,3)\otimes\nu(2,9,1)$	4	76.54%
		$\pi(5,4,2,3)\otimes\nu(2,9,1)$	4	13.82%
16^-	8918	$\pi(6,4,1,3)\otimes\nu(2,9,1)$	4	77.83%
		$\pi(5,4,2,3)\otimes\nu(2,9,1)$	4	9.68%
		$\pi(6,3,2,3)\otimes\nu(2,9,1)$	4	9.56%
17^-	9475	$\pi(6,4,1,3)\otimes\nu(2,9,1)$	4	75.32%
		$\pi(5,4,2,3)\otimes\nu(2,9,1)$	4	11.08%
		$\pi(6,3,2,3)\otimes\nu(2,9,1)$	4	10.51%

possible configurations are considered) were also performed, within the same model space and using the same interaction. The results are illustrated in Fig. 1(b). As seen from the figure the energy agreement between both the restricted calculations and the unrestricted calculations with the experimental value is excellent. In order to evaluate the results from the truncated calculations more thoroughly than is possible with only the energy level comparisons, the wave functions were used to calculate the electromagnetic transition probabilities. The electromagnetic decay properties such as the transition probabilities are a very sensitive test of the wave functions. We have calculated the $BE(2)$ values for a few of the low-lying levels using the wave functions obtained in both the truncated and the full model space. These are compared with the corresponding values obtained by Ji and Wildenthal [12] in Table I. The general agreement between the observed and calculated level energies and the $BE(2)$ values indicates the validity of the truncation scheme. Hence it is possible to internally truncate a large model space by considering only the dominant configurations.

III. SHELL MODEL CALCULATIONS

As mentioned earlier the low-lying levels in $N=50$ nuclei were well described within model spaces which employed an inert neutron core, with the valence protons being restricted to either the $(p_{1/2},g_{9/2})$ or the $(f_{5/2},p_{3/2},p_{1/2},g_{9/2})$ orbits outside ^{88}Sr or ^{78}Ni [1–4] as the valence core. These model spaces were sufficient to explain the level sequences upto a spin of $J=(10-12)\hbar$. However, with the availability of experimental yrast level schemes upto $J\approx25\hbar$, the configuration space to describe the observed level sequences needed to be enlarged. As mentioned earlier to adequately describe the higher angular momentum states the shell model calculations have to be performed within a model space consisting of the $\pi(f_{5/2},p_{3/2},p_{1/2},g_{9/2})$ and $\nu(p_{1/2},g_{9/2},d_{5/2})$ orbits, since these states are expected to be dominated either by the excitations of protons within the fpg subspace coupled to a closed $N=50$ neutron core or by the excitation of a neutron across the $N=50$ core coupled to the protons in the fpg subspace. A calculation of the high spin states assuming single-neutron excitation to the $d_{5/2}$ orbit across the $N=50$ shell closure was performed by Muto *et al.* [13]. The calculations fairly reproduced the observed yrast level structure in ^{94}Ru.

A. Model space and residual interaction

The model space utilized in the calculation includes four proton orbits $(f_{5/2},p_{3/2},p_{1/2},g_{9/2})$ and six neutron orbits $(p_{1/2},g_{9/2},g_{7/2},d_{5/2},d_{3/2},s_{1/2})$. This model space was code named GWB in the code OXBASH [11]. It has ^{66}Ni ($Z=28$, $N=38$) as the inert core. Since an empirical Hamiltonian for this configuration is not available, it was necessary to combine different empirical Hamiltonians with results obtained from schematic nuclear interactions.

The 974 two-body matrix elements for this model space were first derived from the bare G matrix of Hosaka *et al.* [14]. In the second step the various two-body matrix elements obtained from the schematic calculations were replaced by empirically or experimentally determined values (if these were available). The effective interaction for the $\pi(f_{5/2},p_{3/2},p_{1/2},g_{9/2})$ orbits was taken from the work of Ji and Wildenthal [4]. The proton-neutron interactions connecting the $\pi(p_{1/2},g_{9/2})$ and the $\nu(d_{5/2},s_{1/2})$ orbits were taken from the work of Gloeckner [15]. The interaction elements for the $\pi(p_{1/2},g_{9/2})$ and the $\nu(p_{1/2},g_{9/2})$ orbits were taken from the work of Serduke, Lawson, and Gloeckner [16]. The

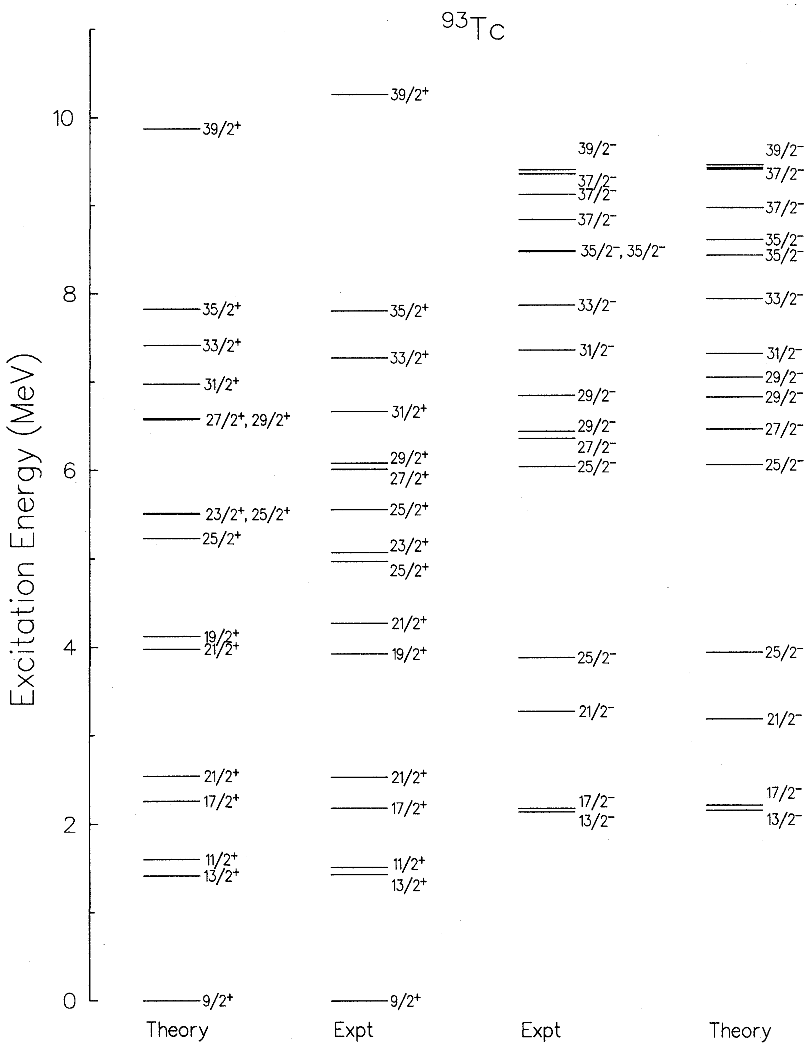

FIG. 3. Comparison of the observed and calculated excitation energies (up to $J=39/2\hbar$) in ^{93}Tc with shell model predictions.

proton-proton interaction elements within the $(p_{1/2},g_{9/2})$ shell were taken from the work of Ball *et al.* [3]. The single-particle energies (in MeV) used were $\epsilon(\pi(f_{5/2}))=-5.322$, $\epsilon(\pi(p_{3/2}))=-6.144$, $\epsilon(\pi(p_{1/2}))=-3.941$, $\epsilon(\pi(g_{9/2}))=-1.250$, $\epsilon(\nu(p_{1/2}))=-0.696$, $\epsilon(\nu(g_{9/2}))=-2.597$, $\epsilon(\nu(g_{7/2}))=5.159$, $\epsilon(\nu(d_{5/2}))=1.830$, $\epsilon(\nu(d_{3/2}))=4.261$, $\epsilon(\nu(s_{1/2}))=1.741$.

B. Configuration space

Because of the large number of active orbitals (in the GWB model space) a truncation of the model space is necessary to make the calculations feasible. As stated earlier the model space could be internally truncated by performing the calculations for the most dominant configurations. From the results for ^{94}Ru it is quite evident that states up to $J=(10-12)\hbar$ could be described by the redistribution of the valence protons in the fpg subspace, and the neutron core may be assumed to be inert. The excitation of the neutron core is essential for the description of only the higher angular momentum states.

Hence we have considered for the low-lying states partitions arising out of the distribution of the valence protons in the fpg subspace, while the neutron $(p_{1/2})$ and $(g_{9/2})$ shells were kept completely filled, i.e., $\pi(6,4,p1,p2)\otimes\nu_{\rm core}$, $\pi(6,3,p1,p2)\otimes\nu_{\rm core}$, $\pi(6,2,p1,p2)\otimes\nu_{\rm core}$, $\pi(5,4,p1,p2)\otimes\nu_{\rm core}$, $\pi(5,3,p1,p2)\otimes\nu_{\rm core}$, $\pi(5,2,p1,p2)\otimes\nu_{\rm core}$, $\pi(4,4,p1,p2)\otimes\nu_{\rm core}$, $\pi(4,3,p1,p2)\otimes\nu_{\rm core}$, where $\nu_{\rm core}=\nu((p_{1/2})^2,(g_{9/2})^{10},(g_{7/2})^0,(d_{5/2})^0,(d_{3/2})^0,(s_{1/2})^0)$, $p1,p2$ correspond to the number of protons in the $p_{1/2},g_{9/2}$ orbits, and the first two numbers correspond to the number of protons in the $f_{5/2}$ and $p_{3/2}$ orbits, respectively.

The influence of this truncation scheme on the excitation energies of the low-lying levels up to $J=13\hbar$ in ^{94}Ru is demonstrated in Fig 1(c). In these calculations the neutron core is assumed to be inert. The $BE(2)$ values using the wave functions obtained in the GWB model space are compared with the values obtained by Ji and Wildenthal in Table I. The agreement between the excitation energies and the $BE(2)$ values is excellent. The comparison we have presented indicates the validity of the truncation scheme developed which has made such large basis shell model calculations possible.

The states above $J=(12-13)\hbar$ are expected to be dominated by the excitation of a single $(g_{9/2})$ neutron across the

TABLE III. Main partitions of wave functions for ^{93}Tc. Each partition is of the form $P=[\pi(p(1),p(2),p(3),p(4))\otimes\nu(n(1),n(2),n(3))]$, where $p(i)$ represents the number of protons occupying the $f_{5/2}$, $p_{3/2}$, $p_{1/2}$, and $g_{9/2}$ orbits, and $n(j)$ represents the number of neutrons in the $p_{1/2}$, $g_{9/2}$, and $d_{5/2}$ orbits, respectively. In these calculations no neutrons were allowed to be excited to the $g_{7/2}$, $d_{3/2}$, and $s_{1/2}$ orbits.

J ($\hbar$)	Energy (keV)	Wave function π	Seniority ν	Partitions (%)
$13/2^+$	1434	$\pi(6,4,2,3)\otimes\nu(2,10,0)$	1	81.25%
		$\pi(6,4,0,5)\otimes\nu(2,10,0)$	1	10.00%
$11/2^+$	1516	$\pi(6,4,2,3)\otimes\nu(2,10,0)$	1	81.25%
$17/2^+$	2184	$\pi(6,4,2,3)\otimes\nu(2,10,0)$	1	81.08%
$21/2^+$	2534	$\pi(6,4,2,3)\otimes\nu(2,10,0)$	1	81.33%
$19/2^+$	3927	$\pi(5,4,1,5)\otimes\nu(2,10,0)$	3	85.08%
		$\pi(5,3,2,5)\otimes\nu(2,10,0)$	3	10.58%
$21/2^+$	4275	$\pi(6,4,0,5)\otimes\nu(2,10,0)$	3	43.56%
		$\pi(5,4,1,5)\otimes\nu(2,10,0)$	3	23.75%
		$\pi(4,4,2,5)\otimes\nu(2,10,0)$	1	10.00%
$25/2^+$	4973	$\pi(5,4,1,5)\otimes\nu(2,10,0)$	3	42.32%
		$\pi(6,4,0,5)\otimes\nu(2,10,0)$	3	30.66%
$23/2^+$	5076	$\pi(6,4,2,3)\otimes\nu(2,9,1)$	3	86.34%
$25/2^+$	5564	$\pi(5,4,1,5)\otimes\nu(2,10,0)$	3	78.88%
		$\pi(5,3,2,5)\otimes\nu(2,10,0)$	3	15.09%
$27/2^+$	6016	$\pi(6,4,2,3)\otimes\nu(2,9,1)$	3	39.74%
$29/2^+$	6087	$\pi(6,4,2,3)\otimes\nu(2,9,1)$	3	93.90%
$31/2^+$	6669	$\pi(6,4,2,3)\otimes\nu(2,9,1)$	3	88.05%
$33/2^+$	7281	$\pi(6,4,2,3)\otimes\nu(2,9,1)$	3	84.91%
$35/2^+$	7811	$\pi(6,4,2,3)\otimes\nu(2,9,1)$	3	83.64%
$39/2^+$	10271	$\pi(5,4,1,5)\otimes\nu(2,9,1)$	5	97.71%
$13/2^-$	2145	$\pi(6,4,1,4)\otimes\nu(2,10,0)$	1	75.99%
		$\pi(5,4,2,4)\otimes\nu(2,10,0)$	1	15.36%
$17/2^-$	2184	$\pi(6,4,1,4)\otimes\nu(2,10,0)$	1	85.94%
$21/2^-$	3280	$\pi(6,4,1,4)\otimes\nu(2,10,0)$	1	70.67%
		$\pi(5,4,2,4)\otimes\nu(2,10,0)$	1	14.84%
$25/2^-$	3887	$\pi(6,4,1,4)\otimes\nu(2,10,0)$	1	86.28%
$25/2^-$	6052	$\pi(5,4,2,4)\otimes\nu(2,9,1)$	3	47.92%
		$\pi(6,4,1,4)\otimes\nu(2,9,1)$	3	46.82%
$27/2^-$	6372	$\pi(5,4,2,4)\otimes\nu(2,9,1)$	3	50.03%
		$\pi(6,4,1,4)\otimes\nu(2,9,1)$	3	44.93%
$29/2^-$	6453	$\pi(5,4,2,4)\otimes\nu(2,9,1)$	3	79.00%
		$\pi(6,4,1,4)\otimes\nu(2,9,1)$	3	16.19%
$29/2^-$	6856	$\pi(6,4,1,4)\otimes\nu(2,9,1)$	3	71.24%
		$\pi(5,4,2,4)\otimes\nu(2,9,1)$	3	19.59%
$31/2^-$	7372	$\pi(5,4,2,4)\otimes\nu(2,9,1)$	3	74.97%
		$\pi(6,4,1,4)\otimes\nu(2,9,1)$	3	20.86%
$33/2^-$	7879	$\pi(5,4,2,4)\otimes\nu(2,9,1)$	3	53.96%
		$\pi(6,4,1,4)\otimes\nu(2,9,1)$	3	38.03%
$35/2^-$	8486	$\pi(5,4,2,4)\otimes\nu(2,9,1)$	3	72.41%
		$\pi(6,4,1,4)\otimes\nu(2,9,1)$	3	24.39%
$35/2^-$	8496	$\pi(5,4,2,4)\otimes\nu(2,9,1)$	3	64.84%
		$\pi(6,4,1,4)\otimes\nu(2,9,1)$	3	29.47%
$37/2^-$	8851	$\pi(6,4,1,4)\otimes\nu(2,9,1)$	3	47.65%
		$\pi(5,4,2,4)\otimes\nu(2,9,1)$	3	42.15%
$37/2^-$	9138	$\pi(6,4,1,4)\otimes\nu(2,9,1)$	3	55.83%
		$\pi(5,4,2,4)\otimes\nu(2,9,1)$	3	34.65%
$37/2^-$	9371	$\pi(5,4,2,4)\otimes\nu(2,9,1)$	3	50.67%
		$\pi(6,4,1,4)\otimes\nu(2,9,1)$	3	43.46%
$39/2^-$	9419	$\pi(6,4,1,4)\otimes\nu(2,9,1)$	3	65.81%
		$\pi(5,4,2,4)\otimes\nu(2,9,1)$	3	27.62%

$N=50$ shell closure into the next major oscillator shell into the $(d_{5/2})$ orbit]. The coupling of the $\nu((g_{9/2})^{-1},(d_{5/2})^1)$ configuration to the protons in the fpg subspace would lead to dimensions of the Hamiltonian matrices which could not be handled within the present computational resources. The model space is internally truncated by including only the following partitions: $\pi(6,4,p1,p2)\otimes(\nu_{\rm core})'$, $\pi(5,4,p1,p2)\otimes(\nu_{\rm core})'$, where $(\nu_{\rm core})' = \nu((p_{1/2})^2,(g_{9/2})^{-1},(g_{7/2})^0,(d_{5/2})^1,(d_{3/2})^0,(s_{1/2})^0)$, $p1,p2$ correspond to the number of protons in the $p_{1/2},g_{9/2}$ orbits, and the first two numbers correspond to the number of protons in the $f_{5/2}$ and $p_{3/2}$ orbits, respectively. The results using these partitions will be discussed in the subsequent sections. However, in our present calculations no particles would be allowed to occupy the $(g_{7/2},d_{3/2},s_{1/2})$ orbits.

IV. RESULTS AND DISCUSSIONS

A. ^{92}Mo

Singh *et al.* [6] studied the level structure of ^{92}Mo up to spins of $I=12^+$ and 17^-. They performed shell model calculations for ^{92}Mo using ^{88}Sr as the core and the $(p_{1/2},g_{9/2})$ valence proton orbits. Spherical shell model calculations using ^{88}Sr as the core and the $(p_{1/2},g_{9/2})$ model space could reproduce the experimental spectra reasonably well up to spins of $I=12^+,11^-$. States above $I=11^-$ could not be generated within the small configuration space used. On the basis of a stretched coupling scheme, where a $d_{5/2}$ neutron was coupled to the ^{91}Mo core, Singh *et al.* were able to attribute the states above $I=12^-$ to be dominated by the excitation of the neutron across the $N=50$ shell gap. A point worth mentioning is that this scheme was able to explain the $I=15^-,16^-,17^-$ group of states only. When this scheme was extended to the group of states from $I=12^-$ to 14^-, it showed considerable deviation from the observed values.

A comparison of the experimental and calculated levels of ^{92}Mo is shown in Fig. 2. The calculations were carried out in the large configuration space GWB described in the earlier section. The excitation energies of all the experimentally known yrast states (except $I=14^-$) are reproduced in the calculations. The main components of the wave functions of the states are shown in Table II. The states with $I\leqslant 12^+,11^-$ are dominated by the excitations of protons within the $\pi(p_{1/2},g_{9/2})$ orbits. The $I=10^+$ and 12^+ states did have a significant contribution from the excitations of protons from the $(f_{5/2},p_{3/2})$ orbits into the $g_{9/2}$ orbit. These configurations were neglected by Singh *et al.* in their calculations. The exclusion of these important configurations resulted in the energy agreement (between the experimental and predicted values) for the $I=10^+$ and 12^+ states, being less perfect as compared to the other low-lying levels. This is attributed to the well-known property of the shell model that the truncation (omission of certain configurations) of a model space renders the ground state less bound [17]. Consequently the predicted excitation energies are higher than the experimental value. The degree of discrepancy between the two is dependent on the contribution of the neglected configurations to the wave function of the state. Omission of a dominant configuration would result in the predicted excitation energies being considerably higher than the experimental value. As seen from Table II the configurations in-

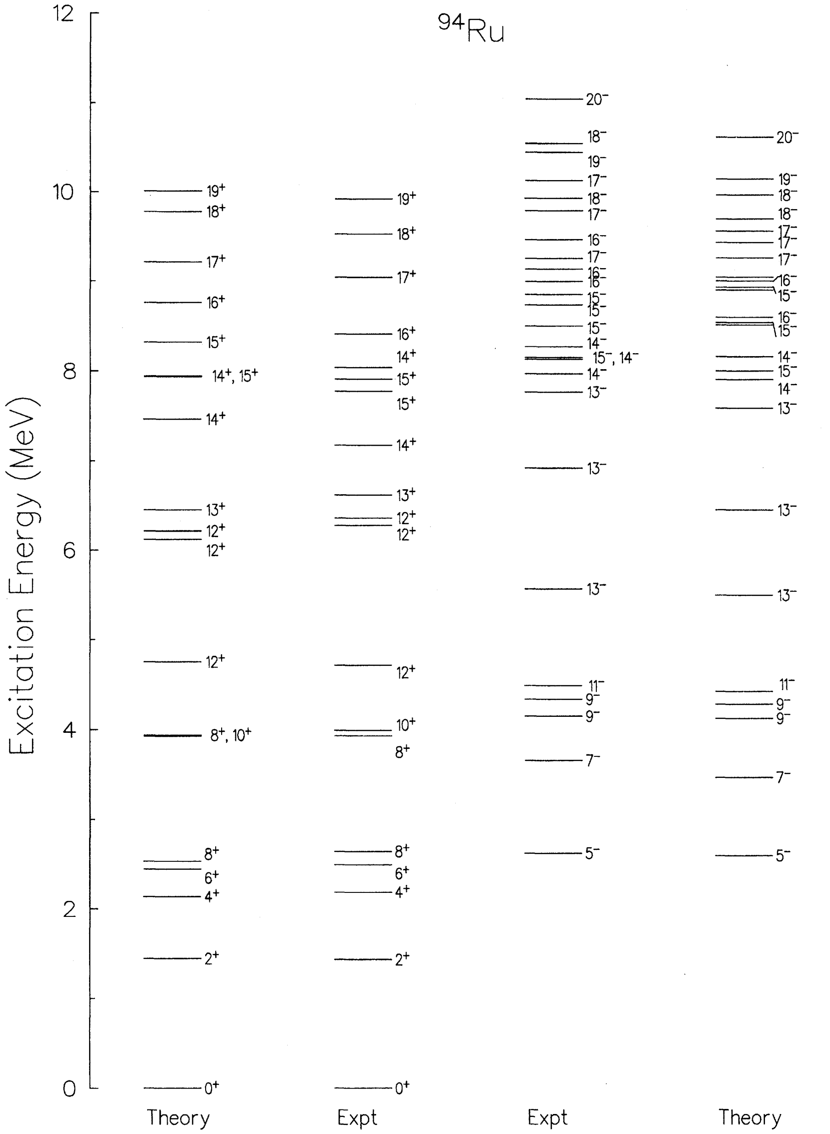

FIG. 4. Comparison of the observed states in ^{94}Ru with spherical shell model calculations (up to $I=19^+,20^-$).

volving the excitation of the protons from the $(f_{5/2},p_{3/2})$ orbits contribute significantly ($\approx$ 20–30 %) to the wave function of the $I=10^+,12^+$ states. Hence the omission of these configurations resulted in the predicted excitation energies being larger than the experimental value.

The $I=12^-,13^-$ states did not have any contribution from the excitation of a $g_{9/2}$ neutron across the $N=50$ shell gap, as stated by Singh *et al.* [6]. These states are dominated by the $\pi((f_{5/2})^{-1}),(p_{3/2})^4,(p_{1/2})^2,(g_{9/2})^3)$ configurations as indicated in Table II. Our calculations could not reproduce the $I=14^-$ state. States with $I=15^-,16^-,17^-$ are dominated by the excitation of a single neutron across the $N=50$ core, i.e., $\nu((g_{9/2})^{-1},(d_{5/2})^1)\otimes\pi((p_{1/2})^1,(g_{9/2})^3)$ configurations. A point worth mentioning is that these states did have a significant contribution from the configurations involving the coupling of the neutron particle-hole excitation across the $N=50$ shell gap to the protons in the fpg subspace.

The agreement between the experimental excitation energies and the shell model predictions for ^{92}Mo indicate single-particle nature of the observed yrast level structure at high spin ($J\approx 17\hbar$ and $E_x\approx 10$ MeV). The excitation of a single neutron across the $N=50$ core adequately describes the observed higher angular momentum states.

B. ^{93}Tc

A high spin structure of ^{93}Tc was reported by Ghugre *et al.* [7,18] and Roth *et al.* [8] up to $I=43/2$ in both the positive and negative parity bands. Ghugre *et al.* described the observed structure of ^{93}Tc within the shell model framework [7,18]. The calculations [18] were performed assuming the excitation of a single neutron across the $N=50$ shell closure. The observed level structures above $I=25/2$ could be adequately described by the excitation of a single neutron across the $N=50$ gap. In view of the additional information available from the work of Roth *et al.* [8], we compare the results of our calculations (using the model space and effective interactions described in the earlier section) with the

TABLE IV. Main partitions of wave functions for ^{94}Ru. Each partition is of the form $P=[\pi(p(1),p(2),p(3),p(4))\otimes\nu(n(1),n(2),n(3))]$, where $p(i)$ represents the number of protons occupying the $f_{5/2}$, $p_{3/2}$, $p_{1/2}$, and $g_{9/2}$ orbits, and $n(j)$ represents the number of neutrons in the $p_{1/2}$, $g_{9/2}$, and $d_{5/2}$ orbits, respectively. In these calculations no neutrons were allowed to be excited to the $g_{7/2}$, $d_{3/2}$, and $s_{1/2}$ orbits.

J ($\hbar$)	Energy (keV)	Wave function π	Seniority ν	Partitions (%)
2^+	1431	$\pi(6,4,2,4)\otimes\nu(2,10,0)$	0	77.03%
		$\pi(6,4,0,6)\otimes\nu(2,10,0)$	0	11.63%
4^+	2187	$\pi(6,4,2,4)\otimes\nu(2,10,0)$	0	76.92%
		$\pi(6,4,0,6)\otimes\nu(2,10,0)$	0	11.56%
6^+	2498	$\pi(6,4,2,4)\otimes\nu(2,10,0)$	0	79.6
		$\pi(6,4,0,6)\otimes\nu(2,10,0)$	0	11.06%
8^+	2644	$\pi(6,4,2,4)\otimes\nu(2,10,0)$	0	78.58%
		$\pi(6,4,0,6)\otimes\nu(2,10,0)$	0	11.56
8^+	3930	$\pi(6,4,2,4)\otimes\nu(2,10,0)$	0	89.68%
10^+	3991	$\pi(6,4,2,4)\otimes\nu(2,10,0)$	0	88.83%
12^+	4716	$\pi(6,4,2,4)\otimes\nu(2,10,0)$	0	91.40%
12^+	6275	$\pi(6,4,0,6)\otimes\nu(2,10,0)$	0	41.99%
		$\pi(5,4,1,6)\otimes\nu(2,10,0)$	2	30.24%
12^+	6358	$\pi(5,4,1,6)\otimes\nu(2,10,0)$	2	78.30%
		$\pi(5,3,2,6)\otimes\nu(2,10,0)$	2	10.50%
14^+	7175	$\pi(6,4,2,4)\otimes\nu(2,9,1)$	2	90.44%
15^+	7773	$\pi(6,4,2,4)\otimes\nu(2,9,1)$	2	89.72%
15^+	7910	$\pi(6,4,2,4)\otimes\nu(2,9,1)$	2	96.20%
14^+	8038	$\pi(6,4,2,4)\otimes\nu(2,9,1)$	2	89.29%
16^+	8411	$\pi(6,4,2,4)\otimes\nu(2,9,1)$	2	95.64%
17^+	9041	$\pi(6,4,2,4)\otimes\nu(2,9,1)$	2	95.84%
18^+	9526	$\pi(6,4,2,4)\otimes\nu(2,9,1)$	2	96.06%
19^+	9920	$\pi(6,4,2,4)\otimes\nu(2,9,1)$	2	95.86%
5^-	2624	$\pi(6,4,1,5)\otimes\nu(2,10,0)$	2	88.50%
7^-	3658	$\pi(6,4,1,5)\otimes\nu(2,10,0)$	2	64.39%
		$\pi(5,4,2,5)\otimes\nu(2,10,0)$	2	23.02%
9^-	4149	$\pi(6,4,1,5)\otimes\nu(2,10,0)$	2	79.27%
		$\pi(5,4,2,5)\otimes\nu(2,10,0)$	2	11.81%
9^-	4338	$\pi(6,4,1,5)\otimes\nu(2,10,0)$	2	89.57%
11^-	4489	$\pi(6,4,1,5)\otimes\nu(2,10,0)$	2	86.01%
13^-	5568	$\pi(6,4,1,5)\otimes\nu(2,10,0)$	2	68.83%
		$\pi(5,4,2,5)\otimes\nu(2,10,0)$	2	22.22%
14^-	7970	$\pi(5,4,2,5)\otimes\nu(2,9,1)$	2	68.83%
		$\pi(5,4,2,5)\otimes\nu(2,9,1)$	2	22.22%
15^-	8133	$\pi(5,4,2,5)\otimes\nu(2,9,1)$	4	89.63%
14^-	8152	$\pi(6,4,1,5)\otimes\nu(2,9,1)$	2	88.01%
		$\pi(6,3,2,5)\otimes\nu(2,9,1)$	4	11.01% 0%
14^-	8272	$\pi(6,4,1,5)\otimes\nu(2,9,1)$	4	88.48%
		$\pi(6,3,2,5)\otimes\nu(2,9,1)$	4	10.36%
15^-	8501	$\pi(5,4,2,5)\otimes\nu(2,9,1)$	4	53.11% %
		$\pi(6,4,1,5)\otimes\nu(2,9,1)$	4	58.34%
15^-	8736	$\pi(6,4,1,5)\otimes\nu(2,9,1)$	4	58.34%
		$\pi(5,4,2,5)\otimes\nu(2,9,1)$	4	34.13%
15^-	8853	$\pi(6,4,1,5)\otimes\nu(2,9,1)$	4	60.66%
		$\pi(5,4,2,5)\otimes\nu(2,9,1)$	4	29.26%
16^-	8996	$\pi(6,4,1,5)\otimes\nu(2,9,1)$	4	85.38%
		$\pi(6,3,2,5)\otimes\nu(2,9,1)$	4	13.20%
16^-	9134	$\pi(6,4,1,5)\otimes\nu(2,9,1)$	4	88.91%
17^-	9254	$\pi(6,4,1,5)\otimes\nu(2,9,1)$	4	86.73%
		$\pi(6,3,2,5)\otimes\nu(2,9,1)$	4	11.76%
16^-	9464	$\pi(6,4,1,5)\otimes\nu(2,9,1)$	4	88.55%
17^-	9787	$\pi(6,4,1,5)\otimes\nu(2,9,1)$	4	92.97%
		$\pi(6,3,2,5)\otimes\nu(2,9,1)$	4	11.76%
18^-	9928	$\pi(6,4,1,5)\otimes\nu(2,9,1)$	4	91.16%
17^-	10129	$\pi(6,4,1,5)\otimes\nu(2,9,1)$	4	86.33%
		$\pi(6,3,2,5)\otimes\nu(2,9,1)$	4	11.83%
19^-	10444	$\pi(6,4,1,5)\otimes\nu(2,9,1)$	4	83.85%
		$\pi(6,3,2,5)\otimes\nu(2,9,1)$	4	15.91%
18^-	10544	$\pi(6,4,1,5)\otimes\nu(2,9,1)$	4	79.85%
		$\pi(6,3,2,5)\otimes\nu(2,9,1)$	4	19.86%
20^-	11042	$\pi(6,4,1,5)\otimes\nu(2,9,1)$	4	92.16%

experimental level scheme reported by Roth *et al.* [8]. Figure 3 displays a comparison of the experimental [8] and theoretical excitation scheme of ^{93}Tc up to $J=39/2\hbar$. The main components of the wave functions are shown in Table III.

The states up to $J=25/2\hbar$ ($E_x\approx$ 5 MeV) are dominated by the protons within the ($f_{5/2}$,$p_{3/2}$,$p_{1/2}$,$g_{9/2}$) orbits. The excitation energies predicted by the present calculation are in better agreement with the experimental values as compared with the calculations of Sinatkas *et al.* [5]. Sinatkas *et al.* [5] predicted that the $I=13/2^-$, $17/2^-$, $21/2^-$, $25/2^-$, and the $25/2^+$ states would be dominated by the $\pi((p_{1/2})^1,(g_{9/2})^4)$ and $\pi((g_{9/2})^5)$ configurations coupled to an inert neutron core, respectively, and hence excluded the contributions from the $\pi(f_{5/2},p_{3/2})$ orbits. As seen from Table III these states were dominated by the $\pi((p_{1/2})^1,(g_{9/2})^4)$ and $\pi((g_{9/2})^5)$ configurations but also had a significant contribution from the excitation of protons from the $f_{5/2}$,$p_{3/2}$ orbits into the $g_{9/2}$ orbit. The omission of these configurations could explain the disagreement between the predictions of Sinatkas *et al.* [5] and the experimental excitation energies. Roth *et al.* [8] erroneously attributed this discrepancy between the predicted and the experimental excitation energies to the large spacing between the $p_{1/2}$ and $g_{9/2}$ single-particle orbits. However, this large energy spacing between the $p_{1/2}$ and $g_{9/2}$ orbits is a well-established experimental observation and is responsible for the $Z=N=40$ being a semimagic number.

Roth *et al.* [8] associated the positive parity states $I=19/2$ at 3.9 MeV, $I=21/2$ at 4.2 MeV, and $I=25/2$ at 5.5 MeV to be dominated by the $\nu((g_{9/2})^{-1},(d_{5/2})^1)$ configurations coupled to the protons in the fpg subspace. Our calculations indicate that these states do not have any contribution from the excitation of a single neutron across the $N=50$ gap. They are dominated by the excitations of protons from the $f_{5/2}$,$p_{3/2}$ orbits into the $g_{9/2}$ orbit, with the neutrons restricted to the ($p_{1/2}$,$g_{9/2}$) orbits. The levels in the positive parity band above $I=27/2$ are dominated by the excitation of a single neutron across the $N=50$ core. The levels from $I=35/2^+$ at 7.8 MeV down to $I=27/2^+$ at 6.0 MeV are

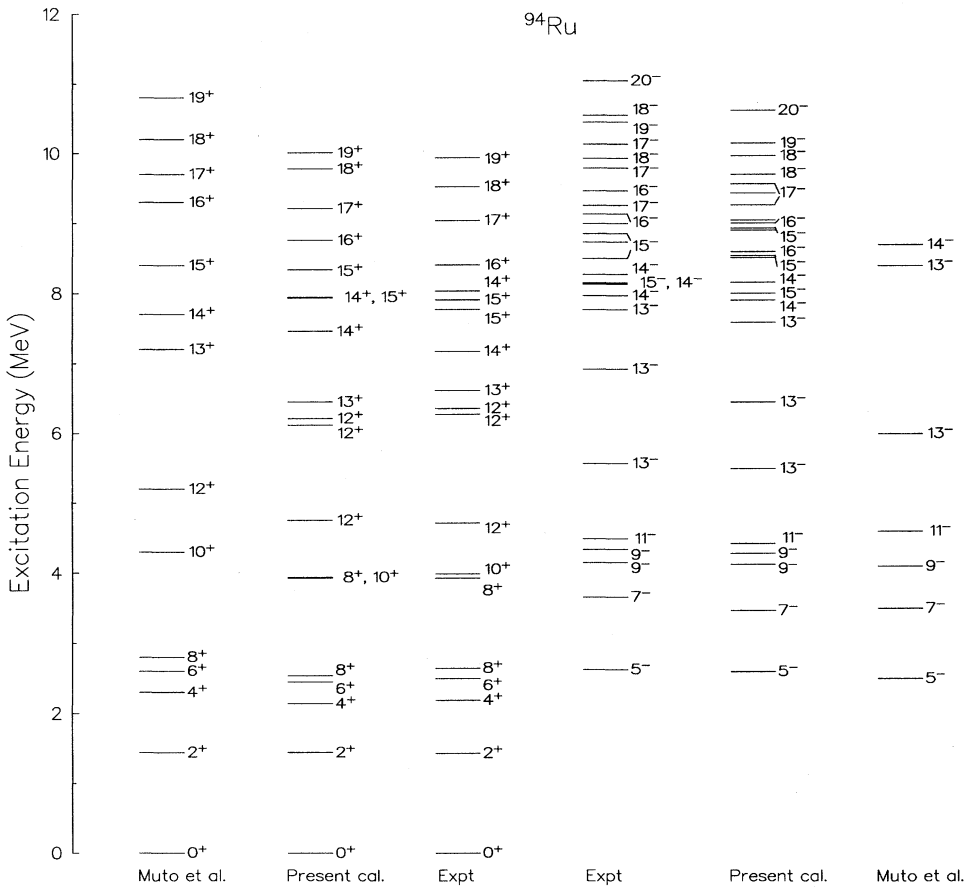

FIG. 5. Comparison of the energy spectra for ^{94}Ru as calculated by Muto *et al.* with the present calculations and the experimental level scheme.

dominated by the $\pi((p_{1/2})^2,(g_{9/2})^3)\otimes\nu((g_{9/2})^{-1},(d_{5/2})^1)$ configuration. The $I=39/2^+$ state at 10.2 MeV is associated with the $\pi((f_{5/2})^5,(p_{3/2})^4,(p_{1/2})^2,(g_{9/2})^5)\otimes\nu((g_{9/2})^{-1},(d_{5/2})^1)$ configuration.

In the negative parity cascade, states from $I=25/2^-$ at 6.0 MeV to $I=39/2^-$ at 9.4 MeV are dominated by the neutron particle-hole excitation across the $N=50$ closed core coupled to the protons in the fpg space. As seen from the table these states are dominated by the $\nu((g_{9/2})^{-1},(d_{5/2})^1)$ configuration coupled to the excitation of protons from the $f_{5/2}$ orbit into the $g_{9/2}$ orbit. This feature is not well understood as one would have expected the $\pi((p_{1/2})^1,(g_{9/2})^4)\otimes\nu((g_{9/2})^{-1},(d_{5/2})^1)$ to be the dominant configuration at higher angular momentum. However, the states at higher excitation energy ($E_x\approx 8.8$ MeV) are dominated by this configuration.

Our calculations were not able to assign any configurations to the states $J\geqslant 39/2$ in both parity bands, due to the nonavailability of detailed experimental data on these states. Thus the higher angular momentum states in ^{93}Tc ($J\geqslant 25/2\hbar$) correspond to the configurations with a neutron particle-hole excitation coupled to the protons in the fpg subspace.

C. ^{94}Ru

The level scheme for ^{94}Ru has been established up to $I=21^+$ and 27^- by Roth *et al.* [8]. Levels up to $I=14^+$ and 15^- were interpreted to be dominated by the protons within the fpg subspace [8] . The levels $12\leqslant I\leqslant 20$ were assumed to be dominated by the excitation of a single neutron across the $N=50$ shell closure, coupled to the protons in the fpg subspace [8]. Levels with spins greater than $J=22$ could be dominated by the excitation of more than one neutron across the $N=50$ shell gap [8].

The calculated and experimental level scheme for ^{94}Ru up to $I=19^+,20^-$ is shown in Fig. 4. The dominant configurations for each angular momentum state are given in Table IV. As seen from the table, the positive parity states up to $I=13^+$ ($E_x=6.6$ MeV) are dominated by the proton excitations within the $(f_{5/2},p_{3/2},p_{1/2},g_{9/2})$ orbits. These states did not have any contribution from the excitation of a neutron across the $N=50$ core. The $I=12^+$ state at 6.3 MeV was assumed to belong to the $\pi((p_{1/2})^2,(g_{9/2})^4)\otimes\nu((g_{9/2})^{-1},(d_{5/2})^1)$ configuration by Roth *et al.* [8]. Our calculations indicate that this state is due to the excitation of a $f_{5/2}$ proton into the $g_{9/2}$ orbit, coupled to an inert neutron $N=50$ core. The levels with $E_x\geqslant 7$ MeV are dominated by the excitation of a single neutron across the $N=50$ core. The levels in the cascade from $J=19^+$ at an excitation energy of 9.9 MeV to $J=14^+$ at 7.1 MeV are dominated by the $\pi((p_{1/2})^2,(g_{9/2})^4)\otimes\nu((g_{9/2})^{-1},(d_{5/2})^1)$ configurations. However, the wave functions of these states had a contribution of about 6% from the proton excitations from the $(f_{5/2},p_{3/2})$ orbits into the $g_{9/2}$ orbits coupled to the

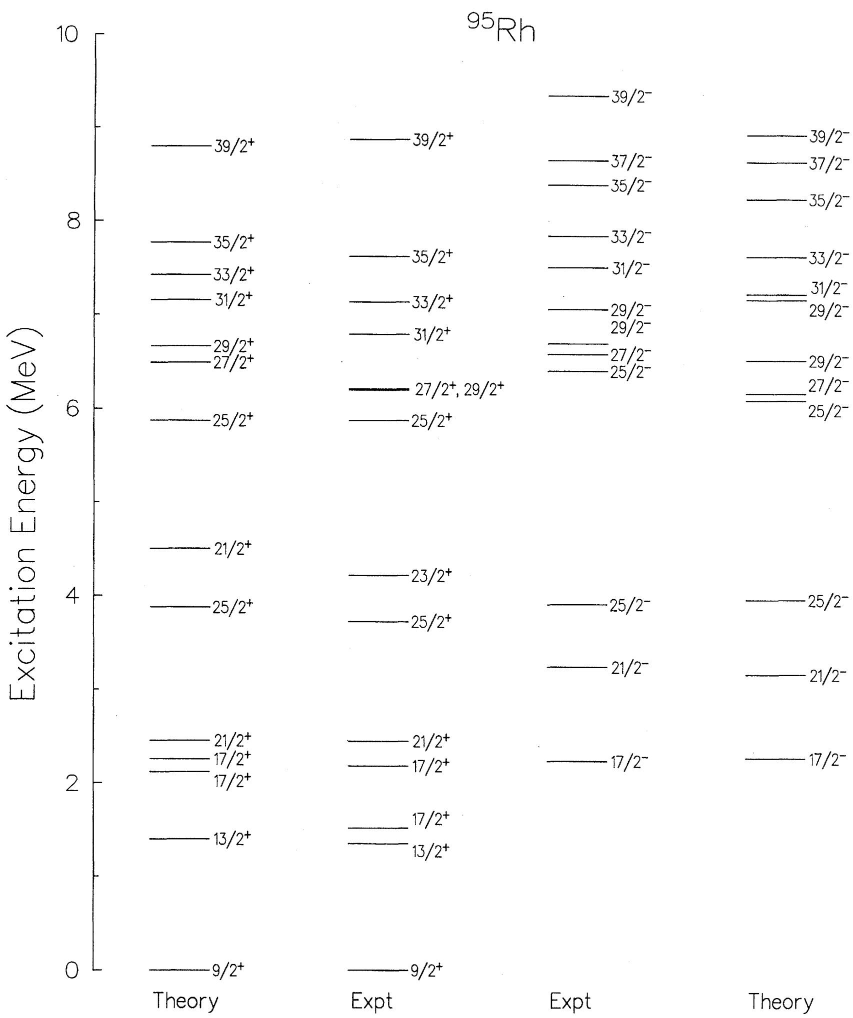

FIG. 6. Comparison of the experimental excitation energies in ^{95}Rh with shell model predictions up to ($J=39/2\hbar$).

$\nu((g_{9/2})^{-1},(d_{5/2})^1)$ configurations. Muto *et al.* [13] had performed the calculations of high spin states in ^{94}Ru assuming the excitation of a single $g_{9/2}$ neutron across the $N=50$ shell into the $d_{5/2}$ orbit. The energy spectra for ^{94}Ru as calculated by Muto *et al.* [13] is compared with the present calculations in Fig. 5. The present calculations are in better agreement with the experimental excitation energies. The calculations of Muto *et al.* [13] reproduced the spacing between the levels, but failed to reproduce the excitation energies. The excitation energies as predicted by Muto *et al.* were higher than the experimental value. This could be attributed to the fact that Muto *et al.* [13] performed the calculations assuming the $\pi((p_{1/2})^2,(g_{9/2})^6) \otimes \nu((g_{9/2})^{-1},(d_{5/2})^1)$ configurations for the high spin states. As stated above these states had a significant contribution ($\approx 6\%$) from the $\nu((g_{9/2})^{-1},(d_{5/2})^1)$ configuration coupled to excitations of the protons from the $(f_{5/2},p_{3/2})$ orbits into the $g_{9/2}$ orbit. The omission of these important configurations resulted in the predicted excitation energies for ^{94}Ru to be higher than the experimental value. A similar feature was seen by us in the calculations of Singh *et al.* [6] and Sinatkas *et al.* [5] for the low-lying levels in ^{92}Mo, ^{93}Tc, and ^{94}Ru. This is attributed to the ground state being rendered less bound, due to the truncation of the model space (omission of important configurations) and consequently the calculated levels are pushed up in excitation energy.

The negative parity states up to $I=13^-$ ($E_x=6.9$ MeV) are dominated by the $\pi((p_{1/2})^1,(g_{9/2})^5)$ configurations. These states also had a contribution of about 6–8 % from the $\pi((f_{5/2})^5,(p_{3/2})^4,(p_{1/2})^2,(g_{9/2})^5)$ configurations coupled to an inert $N=50$ neutron core. The levels with $E_x \geqslant 7.7$ MeV are dominated by the single-neutron excitation into the $d_{5/2}$ shell across the $N=50$ core. These levels are dominated by the $\pi((f_{5/2})^5,(p_{3/2})^4,(p_{1/2})^2,(g_{9/2})^5) \otimes \nu((g_{9/2})^{-1},(d_{5/2})^1)$ configuration. This feature was also observed by us in the negative parity states for ^{93}Tc. We are unable to comprehend this phenomenon at present, since one would have expected these states to be dominated by the $\pi(p_{1/2},g_{9/2} \otimes \nu(g_{9/2})^{-1},(d_{5/2})^1)$ configurations. The calculations of Muto *et al.* [13] were again successful in reproducing the level spacings between the levels, but the predicted levels were higher in excitation energy as compared to the experimental value. This again is attributed to the omission of the configurations involving the $\pi(f_{5/2},p_{3/2})$ orbits which did contribute to the wave functions of these states (about 6%).

The states above $J=19^+$ and 20^- could not be described by our calculations. We agree with Roth *et al.* [8] that the

TABLE V. Main partitions of wave functions for ^{95}Rh. Each partition is of the form $P=[\pi(p(1),p(2),p(3),p(4))\otimes\nu(n(1),n(2),n(3))]$, where $p(i)$ represents the number of protons occupying the $f_{5/2}$, $p_{3/2}$, $p_{1/2}$, and $g_{9/2}$ orbits, and $n(j)$ represents the number of neutrons in the $p_{1/2}$, $g_{9/2}$, and $d_{5/2}$ orbits, respectively. In these calculations no neutrons were allowed to be excited to the $g_{7/2}$, $d_{3/2}$, and $s_{1/2}$ orbits.

J ($\hbar$)	Energy (keV)	Wave function π	Seniority ν	Partitions (%)
$13/2^+$	1351	$\pi(6,4,2,5)\otimes\nu(2,10,0)$	1	88.92%
$17/2^+$	1516	$\pi(6,4,2,5)\otimes\nu(2,10,0)$	1	88.5%
$17/2^+$	2184	$\pi(6,4,2,5)\otimes\nu(2,10,0)$	1	97.56%
$21/2^+$	2448	$\pi(6,4,2,5)\otimes\nu(2,10,0)$	1	90.05%
$25/2^+$	3723	$\pi(6,4,2,5)\otimes\nu(2,10,0)$	1	98.91%
$21/2^+$	4241	$\pi(6,4,0,7)\otimes\nu(2,10,0)$	1	68.75%
$25/2^+$	5874	$\pi(6,4,2,5)\otimes\nu(2,9,1)$	3	98.50%
$27/2^+$	6199	$\pi(6,4,2,5)\otimes\nu(2,9,1)$	3	99.20%
$29/2^+$	6211	$\pi(6,4,2,5)\otimes\nu(2,9,1)$	3	97.60%
$31/2^+$	6794	$\pi(6,4,2,5)\otimes\nu(2,9,1)$	3	96.92%
$33/2^+$	7138	$\pi(6,4,2,5)\otimes\nu(2,9,1)$	3	93.75%
$35/2^+$	7624	$\pi(6,4,2,5)\otimes\nu(2,9,1)$	3	93.87%
$39/2^+$	8874	$\pi(5,4,1,7)\otimes\nu(2,9,1)$	5	85.98%
$17/2^-$	2236	$\pi(6,4,1,6)\otimes\nu(2,10,0)$	1	88.20%
$21/2^-$	3241	$\pi(6,4,1,6)\otimes\nu(2,10,0)$	1	62.36%
		$\pi(5,4,2,6)\otimes\nu(2,10,0)$	1	28.35%
$25/2^-$	3908	$\pi(6,4,1,6)\otimes\nu(2,10,0)$	1	84.37%
$25/2^-$	6404	$\pi(5,4,2,6)\otimes\nu(2,9,1)$	3	88.00%
		$\pi(6,4,1,6)\otimes\nu(2,9,1)$	3	10.08%
$27/2^-$	6585	$\pi(5,4,2,6)\otimes\nu(2,9,1)$	3	95.02%
$29/2^-$	6698	$\pi(5,4,2,6)\otimes\nu(2,9,1)$	3	93.31%
$29/2^-$	7064	$\pi(5,4,2,6)\otimes\nu(2,9,1)$	3	54.29%
		$\pi(6,4,1,6)\otimes\nu(2,9,1)$	3	39.96%
$31/2^-$	7511	$\pi(5,4,2,6)\otimes\nu(2,9,1)$	3	95.67%
$33/2^-$	7845	$\pi(5,4,2,6)\otimes\nu(2,9,1)$	3	81.25%
		$\pi(6,4,1,6)\otimes\nu(2,9,1)$	3	14.38%
$35/2^-$	8394	$\pi(5,4,2,6)\otimes\nu(2,9,1)$	3	62.54%
		$\pi(6,4,1,6)\otimes\nu(2,9,1)$	3	32.15%
$37/2^-$	8655	$\pi(5,4,2,6)\otimes\nu(2,9,1)$	3	78.77%
		$\pi(6,4,1,6)\otimes\nu(2,9,1)$	3	19.08%
$39/2^-$	9346	$\pi(5,4,2,6)\otimes\nu(2,9,1)$	3	91.54%

states with excitation energy of more than 10 MeV could involve the excitation of more than one neutron across the $N=50$ shell gap. Our calculations were able to describe the observed level structure in ^{94}Ru up to an excitation energy of about 10 MeV ($J=20\hbar$) within the shell model framework.

D. ^{95}Rh

Roth *et al.* [8] established the level structure of ^{95}Rh up to $J=43/2^-$, and $47/2^+$. They [8] attributed levels with an excitation energy up to 4 MeV to be dominated by the valence protons within the fpg subspace. The levels having excitation energy between 4 and 10 MeV were supposed to be dominated by the excitation of a single neutron across the $N=50$ core. Roth *et al.* [8] were unable to assign unique configuration assignments to levels above 10 MeV.

Figure 6 displays a comparison of the experimental and theoretical excitation schemes for ^{95}Rh up to $J=39/2\hbar$. The main components of the wave functions are shown in Table V. As seen from the table, states up to an excitation energy of about 5 MeV are dominated by the valence protons within the $(f_{5/2},p_{3/2},p_{1/2},g_{9/2})$ orbits as stated by Roth *et al.* [8]. The positive parity states up to an excitation energy of 4.2 MeV, i.e., the $I=13/2^+,17/2^+,17/2^+,21/2^+,25/2^+,25/2^+$, are dominated by the $\pi((p_{1/2})^2,(g_{9/2})^5)$ configurations. Our calculations indicate that the $I=21/2^+$ state at 4.2 MeV excitation energy does not have any contribution from the neutron core excitation as predicted by Roth *et al.* [8]. The positive parity cascade from $I=39/2^+$ at 8.8 MeV to $I=27/2^+$ at 6.1 MeV is dominated by the excitation of a single neutron across the $N=50$ core. The $\pi((p_{1/2})^2,(g_{9/2})^3)\otimes\nu((g_{9/2})^{-1},(d_{5/2})^1)$ configuration dominates the group of states with $27/2^+\leqslant J\leqslant 35/2^+$ (6.1 MeV$\leqslant E_x\leqslant$ 7.6 MeV). The $I=39/2^+$ state at 8.8 MeV is dominated by the $\pi((f_{5/2})^5,(p_{3/2})^4,(p_{1/2})^1,(g_{9/2})^7)\otimes\nu((g_{9/2})^{-1},(d_{5/2})^1)$ configuration.

The negative parity states up to $I=25/2^-$ ($E_x=3.9$ MeV) are dominated by the $\pi((p_{1/2})^1,(g_{9/2})^6)$ configurations. These states do not have any contribution from the excitation of a single neutron across the $N=50$ core. The states above $I=25/2^-$ ($E_x=6.4$ MeV) to $I=39/2^-$ ($E_x=9.3$ MeV) are dominated by the neutron particle-hole configuration across the $N=50$ shell gap. These states have the $\pi((f_{5/2})^5,(p_{3/2})^4,(p_{1/2})^2,(g_{9/2})^6)\otimes\nu((g_{9/2})^{-1},(d_{5/2})^1)$ as the dominant configuration, a feature which we observed in the negative parity band of ^{93}Tc. We do not understand why the $\pi((p_{1/2})^{1,1},(g_{9/2})^{4,6})\otimes\nu((g_{9/2})^{-1},(d_{5/2})^1)$ configurations do not dominate the higher angular momentum states in ^{93}Tc and ^{95}Rh, respectively, since one would have expected the higher angular momentum states to be dominated by the $\nu((g_{9/2})^{-1},(d_{5/2})^1)\otimes\pi((p_{1/2})^{p1},(g_{9/2})^{p2})$ configurations, where $p1,p2$ denote the number of valence protons outside ^{88}Sr core.

Thus the level structure in ^{95}Rh up to $J=39/2\hbar$ could be understood in terms of the neutron particle-hole excitation across the $N=50$ shell closure coupled to the lower valence proton configurations. Our calculations could not describe the states above $J=39/2$, due to the nonavailability of detailed experimental data on these states. We agree with the conjecture of Roth *et al.* [8] that these states could be due to the excitation of two neutrons across the $N=50$ shell gap.

V. CONCLUSIONS

Within a large model space comprising several valence orbits, the wave function of state would comprise of a large number of configurations due to the distributions of the nucleons in these valence orbits. Of these several configurations the wave function for a particular state would be dominated only by a few configurations. It is possible to internally truncate the large model space by performing the calculations by considering these dominant configurations only.

The level sequences observed in the $N=50$ nuclei ^{92}Mo, ^{93}Tc, ^{94}Ru, and ^{95}Rh are interpreted on the basis of the shell model calculations in the configuration space $(f_{5/2},p_{3/2},p_{1/2},g_{9/2})$ for protons and $(p_{1/2},g_{9/2},g_{7/2},d_{5/2},d_{3/2},s_{1/2})$ for neutrons outside ^{66}Ni as the core. The levels up to an excitation energy of about 4 MeV ($J\approx 12\hbar$) are dominated by the excitation of the protons within the $(f_{5/2},p_{3/2},p_{1/2},g_{9/2})$ orbits. These states did not have any contribution from the excitation of a single neutron across the $N=50$ shell. However, the configurations arising from the excitation of protons from the $(f_{5/2},p_{3/2})$ orbits into the $g_{9/2}$ orbit had to be included to adequately describe even the low-lying states $[J\approx(10-12)\hbar]$ in these $N=50$ nuclei.

The levels with excitation energy between 4 and 10 MeV were dominated by the excitation of a single neutron across the $N=50$ shell gap. These states were dominated by the $\pi((p_{1/2})^{p1},(g_{9/2})^{p2})\otimes\nu((g_{9/2})^{-1},(d_{5/2})^1)$ configurations, where $p1,p2$ denote the number of valence protons in the $p_{1/2},g_{9/2}$ orbits. These states also had a significant contribution from the $\nu((g_{9/2})^{-1},(d_{5/2})^1)$ configuration coupled to the excitations of the protons from the $(f_{5/2},p_{3/2})$ orbits into the $g_{9/2}$ orbit. An exception to this was the negative parity states in ^{93}Tc, ^{94}Ru, and ^{95}Rh which are dominated by the $\pi((f_{5/2})^{-1},(p_{3/2})^4,(p_{1/2})^{p1},(g_{9/2})^{p2})\otimes\nu((g_{9/2})^{-1},(d_{5/2})^1)$ configurations. We have not been able to comprehend this feature. The levels above 10 MeV in excitation energy could not be described by the present calculations. The experimental information is in general not detailed enough to assign any particular configurations to these states. These states could be dominated by the excitation of more than a single neutron across the $N=50$ core.

The present calculations are in better agreement with the experimental excitation energies than the calculations of Sinatkas *et al.* [5] and Muto *et al.* [13]. The reason for the disagreement between the results of Sinatkas *et al.* [5] and Muto *et al.* [13] with the experimental values could be attributed to the omission of the configurations involving protons in the $(f_{5/2},p_{3/2})$ in the calculations.

Hence to adequately describe the observed level structure of the $N=50$ nuclei, within the spherical shell model framework, the model space should encompass a large proton space $[\pi(f_{5/2},p_{3/2},p_{1/2},g_{9/2})$ orbits$]$ and should allow for the excitation of neutrons across the $N=50$ shell closure $[\nu(p_{1/2},g_{9/2},d_{5/2})$ orbits$]$.

To summarize, the higher angular momentum states in the $N=50$ nuclei are dominated by the neutron particle-hole excitation across the $N=50$ shell gap coupled to the lower valence proton configurations. The presence of a gamma ray with $E_\gamma\approx 2$ MeV is a signature of the excitation of a single neutron across the $N=50$ core.

ACKNOWLEDGMENTS

The authors are grateful to Dr. J. A. Sheikh and Dr. H. Herndl for providing us with the shell model code OXBASH. The interest in our work and support from Prof. S. B. Patel and Dr. R. K. Bhowmik are greatly appreciated. One of the authors (S.S.G.) would like to thank Prof. Umesh Garg for his support and hospitality during his stay at Notre Dame. This work was supported by the U.S. National Science Foundation (Grant No. PHY94-02761).

[1] I. Talmi and I. Unna, Nucl. Phys. **19**, 225 (1960).
[2] S. Cohen, R. D. Lawson, M. H. Macfarlane, and M. Soda, Phys. Lett. **10**, 195 (1964).
[3] J. B. Ball, J. B. McGrory, and J. S. Larsen, Phys. Lett. **41B**, 581 (1972).
[4] Xiandong Ji and B. H. Wildenthal, Phys. Rev. C **37**, 1256 (1988).
[5] J. Sinatkas, L. D. Skouras, D. Strottman, and J. D. Vergados, J. Phys. G **18**, 1377 (1992).
[6] Pragya Singh, R. G. Pillay, J. A. Sheikh, and H. G. Devare, Phys. Rev. C **45**, 2161 (1992).
[7] S. S. Ghugre, S. B. Patel, M. Gupta, R. K. Bhowmik, and J. A. Sheikh, Phys. Rev. C **47**, 87 (1993).
[8] H. A. Roth, S. E. Arnell, D. Foltescu, O. Skeppstedt, J. Blomqvist, A. Nilsson, T. Kuroyanagi, S. Mitarai, and J. Nyberg, Phys. Rev. C **50**, 1330 (1994).
[9] M. K. Kabadiyski, F. Cristancho, C. J. Gross, A. Jungclaus, K. P. Lieb, D. Rudolph, H. Garwe, J. Hesse, K.-H. Maier, J.

Eberth, S. S. Koda, W. T. Chow, and E. K. Warburton, Z. Phys. A **343**, 165 (1992).

[10] P. J. Brussard and P. W. M. Glaudemans, *Shell Model Applications in Nuclear Spectroscopy* (North Holland, Amsterdam, 1977).

[11] B. A. Brown, A. Etchegoyen, W. D. M. Rae, and N. S. Godwin, computer code OXBASH, 1984.

[12] Xiandong Ji and B. H. Wildenthal, Phys. Rev. C **38**, 2849 (1988).

[13] K. Muto, T. Shimano, and H. Horie, Phys. Lett. **135B**, 349 (1984).

[14] A. Hosaka, K. I. Kubo, and H. Toki, Nucl. Phys. **A444**, 76 (1985).

[15] D. H. Gloeckner, Nucl. Phys. **A253**, 301 (1975).

[16] F. J. D. Serduke, R. D. Lawson, and D. H. Gloeckner, Nucl. Phys. **A256**, 45 (1976).

[17] E. K. Warburton, J. A. Becker, and B. A. Brown, Phys. Rev. C **41**, 1147 (1990).

[18] S. S. Ghugre, S. B. Patel, and R. K. Bhowmik, Z. Phys. A **349**, 33 (1994).